Proteasome Inhibition Reduces NBR1 Protein Levels in mATG8-Deficient Cells Independently of Lysosomal Degradation and RAB27A

Cristóbal Cerda-Troncoso (1)⚵, Eloísa Arias-Muñoz (1), Gabriela Vargas (1), Belén Gaete-Ramírez (1,2), Karina Cereceda (1), Viviana A. Cavieres (1)§ and Patricia V. Burgos (1,2)§

1. Centro de Biología Celular y Biomedicina CEBICEM, Facultad de Ciencias, Universidad San Sebastián, Avenida del Valle Norte 725, Santiago 8580704, Chile.
2. Centro Científico y Tecnológico de Excelencia Ciencia & Vida, Facultad de Medicina y Ciencia, Universidad San Sebastián, Avenida del Valle Norte 725, Santiago 8580704, Chile.

⚵ Current address
Laboratory for extracellular vesicle research, Department of Human Genetics, KU Leuven. O&N6, Herestraat 49 box 610, 3000 Leuven, Belgium.

§ Corresponding authors
Cavieres VA, email: viviana.cavieres@uss.cl
Burgos PV, email: patricia.burgos@uss.cl

48 **Graphical abstract**

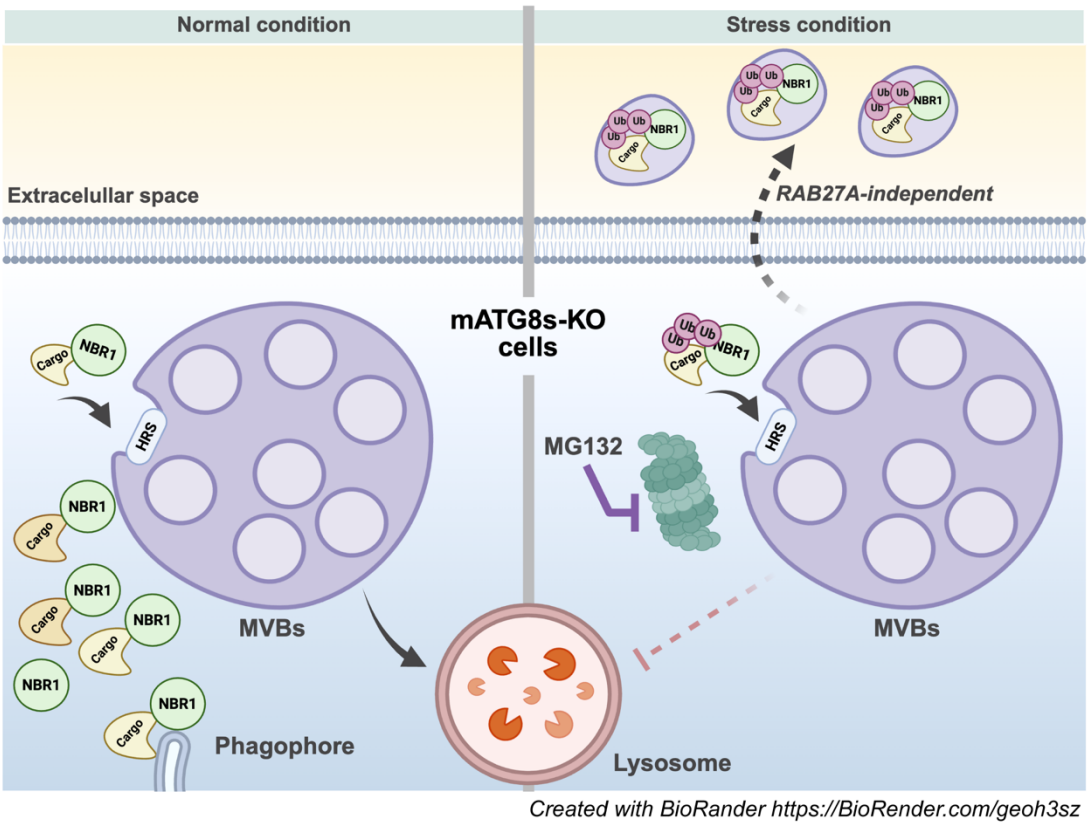

Graphical Abstract
Cerda-Troncoso C, et al., 2025

49
50 *Created with BioRender https://BioRender.com/geoh3sz*
51
52 *In the absence of mATG8s, NBR1 may be recruited to multivesicular bodies (MVBs) via*
53 *HRS, for later degradation in lysosomes (left panel). Under proteasomal inhibition (right*
54 *panel), NBR1 associated with MVBs (with ubiquitinated cargos) is downregulated,*
55 *independent of lysosomes. Possibly, this downregulation is due to a secretion process,*
56 *through a RAB27A-independent mechanism.*
57

Abstract

Autophagy is a lysosome-dependent degradation process that involves autophagosome formation, typically mediated by mammalian ATG8 proteins (mATG8s). Autophagosomes can still form in their absence, suggesting alternative mechanisms. NBR1, a selective autophagy receptor, has been shown to compensate for autophagy defects. Here, we examined NBR1 regulation under proteotoxic stress in mATG8s-deficient HeLa cells. NBR1 levels were elevated in mATG8s knockout (KO) cells under basal conditions but decreased significantly after treatment with the proteasome inhibitor MG132. This reduction was not prevented by lysosomal inhibition with BafA1, indicating a non-lysosomal mechanism. Silencing of RAB27A reduced basal NBR1 levels, and the effects of MG132 were no longer observed, likely due to already diminished NBR1. Remaining NBR1 localized to puncta positive for ubiquitin and the ESCRT-0 component HRS, suggesting involvement of a ubiquitin-dependent endosomal pathway. Overall, our results suggest that under proteotoxic stress and impaired autophagy, cells activate alternative routes, potentially involving unconventional secretion, to regulate NBR1 levels.

Introduction

(Macro)Autophagy is a catabolic process that delivers cytoplasmic components to the lysosome for degradation through double-membrane autophagosomes. Its biogenesis requires the coordinated action of autophagy-related (ATG) proteins. In yeast, ATG8 is essential for autophagosome formation (1), while in mammals, this function is fulfilled by ATG8 orthologs (mATG8s), including LC3 and GABARAP protein families. Notably, unlike yeast, mammals can form autophagosomes even in the absence of mATG8s (2). Selective cargo recognition is mediated by autophagy receptors such as NBR1 and SQSTM1/p62 (3). In the absence of mATG8s, cargo can instead be secreted via autophagy-dependent secretion (4). Notably, NBR1 compensates for the loss of ATG7, an essential protein involved in mATG8s lipidation by promoting autophagosome formation through an alternative mechanism (5).

Given the central role of NBR1 in coordinating selective autophagy and potential compensatory pathways, we explored how NBR1 behaves under conditions of proteasomal inhibition in the absence of mATG8s. For this, HeLa cells, both WT and mATG8s KO, were compared, revealing that mATG8s KO cells displayed elevated levels of NBR1 relative to WT. Surprisingly, proteasomal inhibition with MG132 led to a significant decrease in NBR1 levels in mATG8s KO cells. Inhibiting lysosomal degradation using BafA1 failed to prevent this reduction, suggesting a non-lysosomal mechanism. Moreover, silencing of RAB27A, a GTPase involved in endo-lysosomal vesicle trafficking and secretion, reduced basal NBR1 levels and abolished its further decrease by MG132, likely due to already diminished levels rather than a requirement for RAB27A. Residual NBR1 localized in punctate structures positive for ubiquitin and the ESCRT-0 component HRS, suggesting a ubiquitin-dependent endosomal mechanism. Altogether, these findings suggest that under proteotoxic stress and impaired autophagy, cells engage alternative pathways, potentially involving unconventional secretion of NBR1.

Methods

Reagents and Antibodies

MG132 (cat#47479), Bafilomycin A1 (BafA1, cat#B1793), anti-NBR1 (cat#sc-130380, NBP171703), anti-EEA1 (cat#61045), anti-CD63 (cat#ab8219), anti-Cathepsin D (cat#AF1014), anti-HRS (cat#ab15539), anti-ubiquitin (cat#AUB01), and anti-RAB27A (cat#168013) were used.

Cell Culture, Treatments, and Western Blot

HeLa WT and mATG8s KO cells (courtesy of Dr. Maho Hamasaki, Osaka University), and HEK293T cells (cat#632180), were cultured in DMEM High Glucose (cat#12800-017) supplemented with 10% heat-inactivated FBS (cat#sv30160.03), 100 U/mL penicillin, and 100 µg/mL streptomycin (cat#15070-063), at 37°C and 5% CO_2. Cells were seeded after trypsinization with 0.05% trypsin and 1 mM EDTA (cat#25300-54).

For treatments, cells were incubated with 10 µM MG132 for 8 h or 100 nM BafA1 for 4 h. DMSO was used as vehicle control.

Cells were washed with cold PBS (cat#46-013) and lysed in RIPA buffer [50 mM Tris-HCl, 150 mM NaCl, 5 mM EDTA, 1% NP-40, 1% sodium deoxycholate, 0.1% SDS, pH 7.4] supplemented with protease inhibitors (cat#P8340). Lysates were sonicated on ice (3 pulses, 2–3 s, 40 mA) and processed for SDS-PAGE, Western blotting, and membrane detection following previously described protocols (6).

Immunofluorescence and Confocal Microscopy

Cells grown on coverslips were fixed, permeabilized, and stained as previously described (6). Images were acquired using a Leica TCS SP8 confocal microscope (6).

Lentiviral Transduction and Stable Knockdown

RAB27A knockdown was achieved by lentiviral transduction with shRNA as previously described (6). mATG8s KO cells were selected with 6 µg/mL puromycin (cat#P8833). Knockdown efficiency was confirmed by Western blot.

Data Analysis

Densitometry and image quantification were performed using FIJI (ImageJ), Excel 2022, and Prism 10.0 (macOS). Statistical significance was determined using a one-tailed t-test.

Results

<u>Proteasomal inhibition with MG132 reduces NBR1 levels in HeLa cells lacking mATG8s proteins, independently of lysosomal degradation</u>

The absence of mATG8s in HeLa cells perturbs autophagosome trafficking, alters their morphology, and slows down their biogenesis rate (2), ultimately leading to the accumulation of selective autophagy receptors. Consistent with this, we confirmed the accumulation of NBR1 in mATG8s-KO HeLa cells compared to wild-type (WT) by Western blot analysis (Fig. 1A, lanes 1 and 3; Fig. 1B). Considering that in mATG8s-KO cells, cells may rely on the proteasomal system to maintain proteostasis, where NBR1 can promote

substrate delivery to the proteasome, we explore whether proteasome inhibition increases NBR1 levels. Contrary to our expectations, treatment with 10 µM MG132 for 8 h led to a significant decrease in NBR1 protein levels in mATG8s-KO cells, as shown by Western blot (Fig. 1A line 3 and line 4; Fig. 1B) and immunofluorescence (Fig. 1C and 1D), a phenotype that was not observed in WT cells. Proteasome inhibition is known to activate lysosomal biogenesis and autophagosome degradation (7). We tested whether the reduction in NBR1 levels was due to lysosomal degradation. Cells were treated with 10 µM MG132 for 8 h, with 100 nM BafA1 added during the final 2 h to inhibit lysosomal activity. Lysosomal inhibition did not restore NBR1 levels in mATG8s-KO cells (Fig. 1E and 1F), indicating that the MG132-induced decrease in NBR1 is not mediated by lysosomal degradation.

<u>Residual NBR1 levels in response to catalytic proteasome inhibition co-localize with ESCRT-0 component HRS and Ubiquitin aggregates.</u>

To gain insight into the trafficking pathways involved, we next assessed the subcellular distribution of NBR1 following MG132 treatment. Given that NBR1 can be incorporated into endosomes under basal conditions in yeast (8), we evaluated its co-localization with markers of the endolysosomal pathway in mATG8s-KO cells treated with MG132, including early endosomes (EEA1), the ESCRT-0 component HRS (involved in endosomal sorting (9)), late endosomes (CD63), and lysosomes (Cathepsin D, CathD). Confocal microscopy analysis revealed a significant co-localization of NRB1 with HRS, compared to the other markers (Fig. 2A and 2B), predominantly within large circular structures (Fig. 2A, arrowheads). Since NBR1 recognizes ubiquitinated cargos for degradation, we next examined the co-localization of NBR1 and HRS with ubiquitin following proteasome inhibition in mATG8s-KO cells. Confocal analysis showed that both NBR1 and HRS co-localize with ubiquitin after MG132 treatment (Fig. 2C and 2D), within similar structures.

<u>Proteasomal inhibition with MG132 reduces NBR1 levels in mATG8-KO cells, via a RAB27A-independent mechanism.</u>

Given the observed association between HRS and NBR1 after proteasome inhibition, and that HRS mediates earlier steps in intraluminal vesicle formation at endosomes, later released as exosomes via MVB-plasma membrane fusion regulated by the GTPase RAB27A (9), we investigated whether NBR1 reduction could be mediated by RAB27A-dependent secretion. To test this, we generated stable RAB27A knockdown in mATG8s-KO cells via lentiviral transduction (shRAB27A), using cells expressing a shRNA against luciferase as a control (shLuc). Western blot analysis revealed reduced basal NBR1 levels in shRAB27A compared to shLuc cells (Fig. 2E, lanes 1 and 3; Fig. 2F). We next assessed the effect of proteasome inhibition in these lines. As expected, MG132 treatment reduced NBR1 levels in shLuc cells (Fig. 2E, lanes 1 and 2; Fig. 2F). In contrast, MG132 treatment did not further decrease NBR1 levels in shRab27A cells (Fig. 2E, lanes 3 and 4; Fig. 2F), suggesting that the reduction of NBR1 upon proteasomal inhibition occurs through a RAB27A-independent mechanism.

Discussion

Here, we show that NBR1 protein levels, elevated in mATG8s-KO cells, decrease under two distinct stress conditions: proteasomal inhibition and RAB27A silencing. The

remaining NBR1 signal localizes to dot-like structures that co-localize with the ESCRT-0 component HRS and ubiquitin, suggesting involvement of the ubiquitin-dependent endosomal pathway. Consistent with this, lysosomal inhibition using BafA1 did not restore NBR1 levels, and no intracellular accumulation was observed, supporting the notion that its reduction is not due to lysosomal degradation. RAB27A silencing in mATG8s-KO cells also reduced NBR1 levels, suggesting that in the absence of this GTPase, NBR1 may be rerouted toward degradation or secretion via yet unidentified mechanisms. Although we did not directly assess secretion, our findings align with the possibility that NBR1 is released via a non-canonical pathway under cellular stress. The absence of MG132-induced NBR1 reduction in RAB27A-silenced cells likely reflects already diminished basal levels due to RAB27A depletion, rather than indicating its requirement in the MG132 response. Thus, NBR1 downregulation upon proteasome inhibition likely proceeds through a RAB27A-independent mechanism.

These results suggest that when canonical autophagy is compromised, cells become more vulnerable to additional stressors such as proteasome inhibition or vesicular trafficking disruption. In compensation, they may activate alternative pathways involving selective autophagy receptors that bind ubiquitinated cargo, with HRS potentially contributing. HRS has been implicated in autophagy-dependent secretory autophagy, typically requiring LC3 (10). However, our data point to an LC3-independent mechanism, consistent with the absence of mATG8s, where NBR1 may be redirected into ubiquitin-enriched vesicles. Whether these vesicles are ultimately secreted, and the nature of the underlying pathway, remain to be determined.

Given that aging and chronic proteotoxic stress impair canonical autophagy, identifying alternative routes for protein handling may offer new insights into cellular resilience and protein quality control.

Acknowledgments

We kindly thank to Drs. Manuel Varas-Godoy (Universidad San Sebastián) and Matías Ostrowski (Universidad de Buenos Aires) for providing the plasmids used in lentiviral particle production. We are also grateful to Dr. Nicolás Albornoz for his contribution to the generation of raw ~~~+~data not included in this work.

Fundings

This research was funded by Fondo Nacional de Desarrollo Científico y Tecnológico de Chile (FONDECYT) grants numbers 1211261 (Patricia V. Burgos), and 3220485 (Viviana A. Cavieres); and Vicerrectoria de Investigación y Doctorados, Universidad San Sebastián for PhD scholarship (Cristóbal Cerda-Troncoso).

Author contributions

Conceptualization, **C.C-T.**, **V.A.C** and **P.V.B.**; Methodology, **C.C.T.**, **A.E-M**., **B.G-R.**, **K.C.**, and **V.A.C**; Formal analysis, **C.C-T.**, **A.E-M.**, **V.A.C.**, and **P.V.B.**; Resources, **C.C-T.**, **V.A.C.**, and **P.V.B.**; writing—original draft preparation, **C.C-T.**, **V.A.C.**, and **P.V.B.** writing—review and editing, **C.C-T.**, **V.A.C.**, and **P.V.B.**; funding acquisition, **V.A.C.**, and **P.V.B.**

239
240
241 **Conflict of interest statement**

242 The authors declare no conflict of interest.
243
244 **References**

245 **1.** Nakatogawa H, Ichimura Y, Ohsumi Y. Atg8 controls phagophore expansion during
246 autophagosome formation. Mol Biol Cell. 2008 Jul;19(7):3290-8. doi:
247 10.1091/mbc.E07-12-1292.
248 **2.** Nguyen TN, Padman BS, Usher J, Oorschot V, Ramm G, Lazarou M. Atg8 family
249 LC3/GABARAP proteins are crucial for autophagosome-lysosome fusion but not
250 autophagosome formation during PINK1/Parkin mitophagy and starvation. J Cell
251 Biol. 2016 Dec 19;215(6):857-874. doi: 10.1083/jcb.201607039.
252 **3.** Vargas JNS, Hamasaki M, Kawabata T, Youle RJ, Yoshimori T. The mechanisms and
253 roles of selective autophagy in mammals. Nat Rev Mol Cell Biol. 2023
254 Mar;24(3):167–85. doi:10.1038/s41580-022-00542.
255 **4.** Tan HWS, Luo S, Wang Z, et al. A degradative to secretory autophagy switch
256 mediates mitochondria clearance in the absence of the mATG8-conjugation
257 machinery. Nat Commun. 2022 Jun 28;13:3720. doi: 10.1038/s41467-022-31213-7.
258 **5.** Shoemaker CJ, Huang H, Weir NR, et al. Receptor-mediated clustering of FIP200
259 bypasses the role of LC3 lipidation in autophagy. EMBO J. 2020 Nov
260 23;39(23):e104948. doi: 10.15252/embj.2020104948.
261 **6.** Cerda-Troncoso C, et al. Chemo-small extracellular vesicles released in cisplatin-
262 resistance ovarian cancer cells are regulated by the lysosomal function. J Extracell
263 Vesicles. 2024 May 30; 3(6):e157.. doi: 10.1002/jex2.157
264 **7.** Zhang X, Garstka MA, Wang Z, et al. Proteasome Inhibition Activates Autophagy-
265 Lysosome Pathway and the Formation of Aggresome in Human Mature Dendritic
266 Cells. Front Cell Dev Biol. 2019;7:282. doi: 10.3389/fcell.2019.00282.
267 **8.** Liu XM, Sun LL, Hu W, Ding YH, Dong MQ, Du LL. ESCRTs cooperate with a selective
268 autophagy receptor to mediate vacuolar targeting of soluble cargos. Mol Cell. 2015
269 Sep 17;59(6):1035–42. doi:10.1016/j.molcel.2015.07.034.
270 **9.** Hessvik NP, Llorente A. Current knowledge on exosome biogenesis and release. Cell
271 Mol Life Sci. 2018 Jan;75(2):193-208. doi: 10.1007/s00018-017-2595-9.
272 **10.** Leidal AM, Huang HH, Marsh T, Solvik T, Zhang D, Ye J, Kai F, Goldsmith J, Liu JY,
273 Huang YH, Monkkonen T, Vlahakis A, Huang EJ, Goodarzi H, Yu L, Wiita AP, Debnath
274 J. LC3-dependent EV loading and secretion (LDELS) promotes TFRC secretion and
275 microenvironment remodeling. Nat Cell Biol. 2023 May;25(5):741-754. doi:
276 10.1038/s41556-023-01154-3.

277
278
279
280
281

Figures and legends

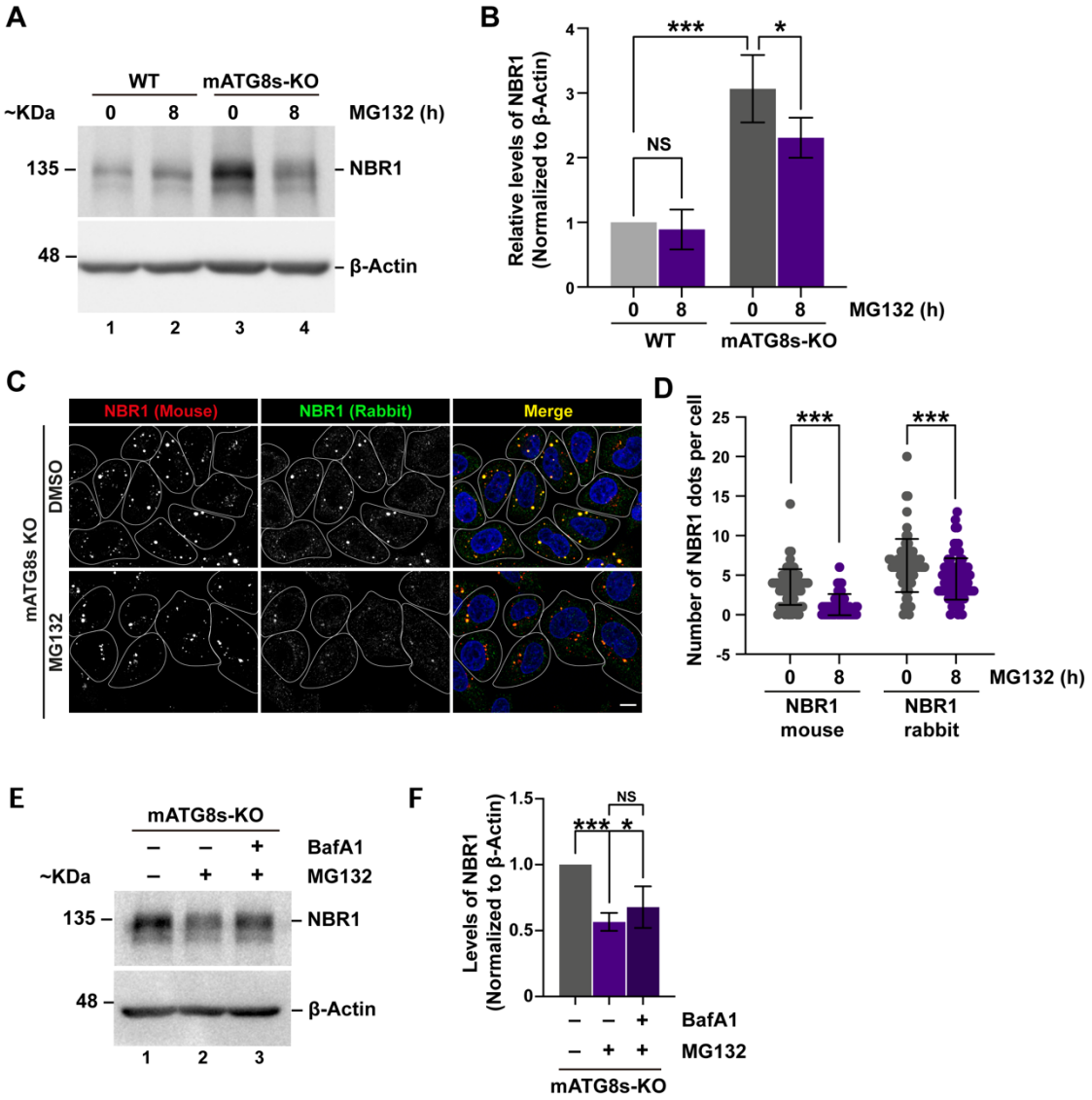

Figure 1
Cerda-Troncoso C, et al., 2025

Figure 1. Catalytic proteasome inhibition reduces NBR1 levels in mATG8-deficient cells. (A) Western blot of endogenous NBR1 and β-actin in HeLa WT and HeLa mATG8s KO cells treated with 10 µM MG132 for 0 or 8 h. Cells were lysed with RIPA buffer. (B) Densitometric quantification of NRB1 levels shown in (A). NS: No-Significative **P<0.01, ***P<0,001; unpaired-parametric t-Test. (C) Immunofluorescence analysis of NBR1 distribution in HeLa WT and HeLa mATG8s-KO cells treated with 10 µM MG132 for 0 or 8 h; Scale bar 10 µm. (D) Quantification of NBR1 positive puncta per cell from images in (C); ***P<0,001; unpaired-parametric t-Test. (E) Western blot of endogenous NBR1 and β-actin in HeLa mATG8s KO cells treated with 10 µM MG132 for 0 or 8 h, with or without 100 nM BafA1 added during the final 2 h. (F) Densitometric quantification of NBR1 levels from (E); NS: No-Significative, *P<0.05, ***P<0.001; unpaired-parametric t-Test.

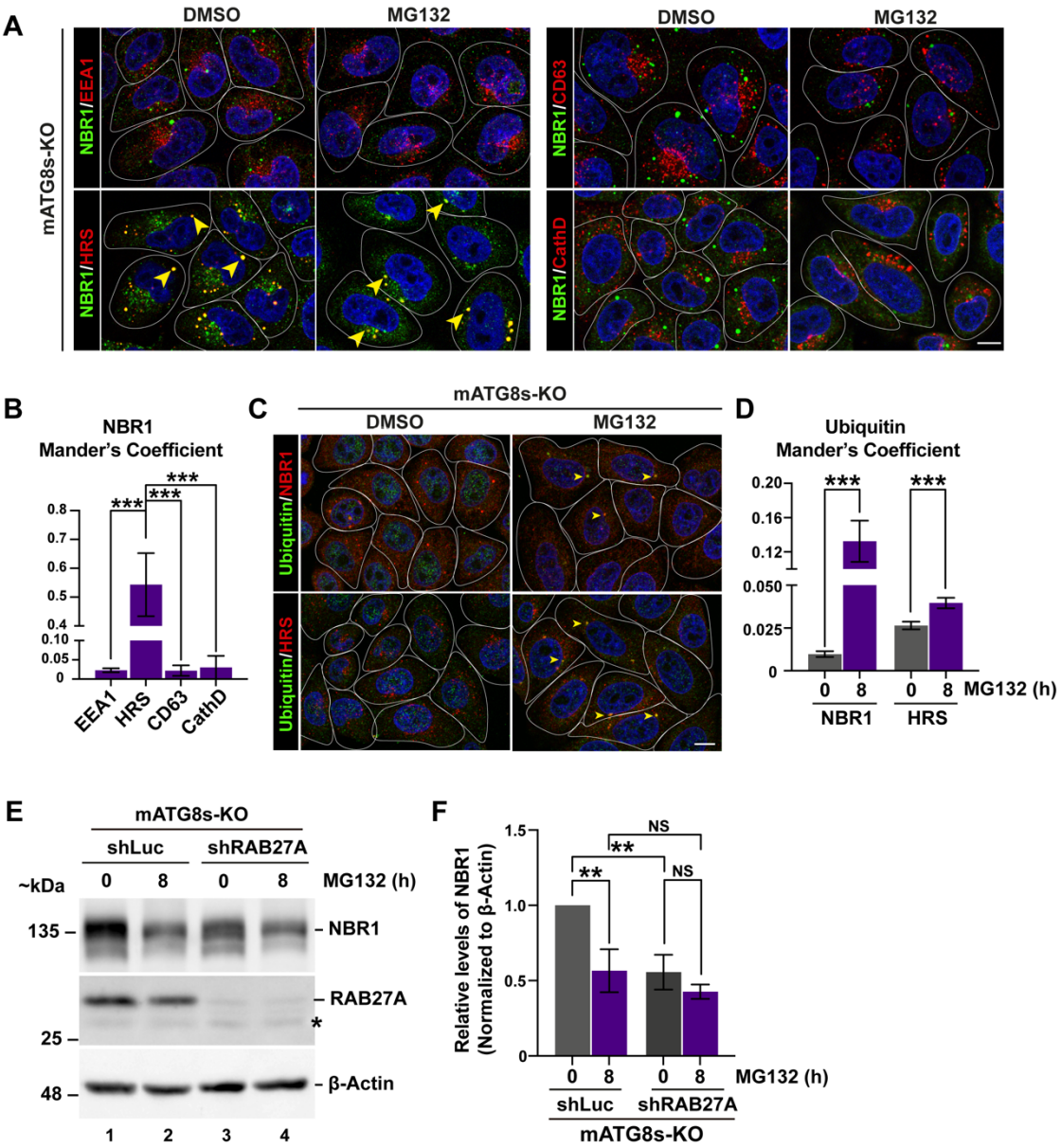

Figure 2
Cerda-Troncoso C, et al., 2025

349
350
351 **Figure 2**. Residual NBR1 localizes to HRS and ubiquitin structures following catalytic
352 proteasome inhibition. (A) Confocal analysis of NBR1 with endolysosomal markers in
353 mATG8s KO cells treated with 10 µM MG132 for 0 or 8 h. Markers include EEA1 (early
354 endosomes), HRS (MVBs), CD63 (secretory MVBs), and CathD (lysosomes); arrowheads
355 indicate areas of co-localization. (B) Representative quantification of NBR1 co-
356 localization with HRS from panel (A). (C) Mander's coefficient quantification of NBR1 co-
357 localization with the indicated endolysosomal markers after MG132 treatment;
358 ***P<0.001; unpaired-parametric t-Test. (D) Confocal analysis of NBR1 or HRS co-
359 localization with ubiquitin after 0 or 8 h of 10 µM MG132 treatment in mATG8s KO cells;
360 arrowheads show co-localization. (D) Mander's coefficient quantification of ubiquitin
361 co-localization with NBR1 or HRS following MG132 treatment as shown in (C);
362 ***P<0.001; unpaired-parametric t-Test. (F) Western blot analysis of NBR1 and β-actin
363 protein levels in mATG8s KO either shLuc and shRAB27A cells, treated with 10 µM
364 MG132 for 0 or 8 h. (G) Densitometric quantification of Western blot shown in (F); NS:
365 No-Significative **P<0.01; unpaired-parametric t-Test.
366